93-164

объединенный
институт
ядерных
исследований
дубна

E2-93-164

S.V.Goloskokov, O.V.Selyugin

SPIN EFFECTS IN HIGH ENERGY QUARK-QUARK SCATTERING

Submitted to «Ядерная физика»

1993

Investigation of spin effects in high energy reactions is a crucial problem of perturbative QCD. The standard perturbative QCD calculations cannot explain such experimentally observable phenomena in hard and soft reactions [1].

(i) In hard processes (all kinematic variables are larger than the dimensional parameters of the process: $s, |t|, |u| \gg m_i^2$) the spin-flip effects are absent in the massless limit [2]. If we do not omit the quark masses, the spin-flip amplitude are suppressed as a power of s with respect to the spin-non-flip one.

$$\frac{|\,T_{flip}\,|}{|\,T_{non-flip}\,|} \simeq \frac{m}{\sqrt{s}}$$

(ii) In high energy reactions at small momenta transfer ($s \to \infty$, t-fixed) the t-channel exchange with vacuum quantum numbers (pomeron) contributes. The calculations of diagrams and their summations are usually performed in the leading logarithmic approximation (see [3] e.g). However the spin-flip amplitudes are absent in this approximation.

Note that there are many spin experimental data at high energies and fixed momenta transfer. So the investigation of the pomeron spin structure is very important. The vacuum t-channel amplitude is usually associated in QCD with the two-gluon exchange [4]. The spinless pomeron was analysed in [5, 6, 7] on the basis of a QCD model with taking account of the nonperturbative properties of the theory. A similar model was used to investigate the spin effects in pomeron exchange. It was shown that different contributions like a gluon ladder [8] and quark loops [9, 10, 11], may lead to the spin-flip amplitude growing as s in the limit $s \to \infty$. As a result the spin-flip amplitudes are suppressed only logarithmically with respect to the spin-non-flip amplitude

$$\frac{|\,T_{flip}\,|}{|\,T_{non-flip}\,|} \simeq \frac{m\sqrt{|t|}}{a(m,t)\,\ln s/s_0}. \tag{1}$$

Here and in what follows $m = .33GeV$ is the constituent quark mass and a is a function linearly dependent on $|t|$ at large $|t|$. This result confirms the absence of the spin-flip amplitudes only in the leading log approximation.

The purpose of this paper is the investigation of the spin effects in quark-quark scattering that plays an important role in different high energy processes. Previously this high-energy subprocess was studied in the soft momentum transfer region. It was shown in [8] within the qualitative QCD analysis that the qq spin-flip amplitude growing as s can be obtained in the α_s^3 order. Such effects in qq scattering were calculated in [12] by the QCD long-distance model with the elements of perturbative theory together with the nonperturbative propagators. In this paper the quantitative calculations of the spin effects in qq scattering will be performed in the α_s^3 order in the semi-hard

region $s \to \infty$, $|t| > 1GeV^2$ where the perturbative theory can be used. To solve this problem, we shall calculate the non-leading log terms of the scattering amplitude omitting only the power corrections of the order $1/s$. The analysis of different matrix structure contributions to the spin-flip amplitude will be done too. Their magnitudes are not very small but they are strongly compensated for quarks on the mass-shell. The factorization of the spin-flip amplitude into the spin-dependent large-distance part and the high-energy spinless pomeron will be shown. This permits us to discuss the possible results of summation of the pomeron graphs in higher orders of QCD in the spin-flip contributions.

Let us investigate the quark-quark scattering

$$q(p_1) + q(p_2) = q(p_3) + q(p_4).$$

In what follows we shall use the symmetric coordinate system in which the sum of quark momenta before and after scattering is directed along the z-axis

$$p = \frac{p_1 + p_3}{2} = (p_0, 0, 0, p_z),\ p' = \frac{p_2 + p_4}{2} = (p_0, 0, 0, -p_z);$$

and the momenta transfer Δ, along x-axis [8]

$$r = \frac{p_1 - p_3}{2} = \frac{p_4 - p_2}{2} = (0, -\Delta/2, 0, 0).$$

As a result

$$p^2 = p'^2 = m^2 + \frac{\Delta^2}{4},\ (pr) = (p'r) = 0,\ s \simeq 2(pp').$$

It is well known that the spin-flip amplitude growing as s is absent in the born two-gluon diagrams. This contribution can be obtained from more complicated ladder diagrams. We shall investigate the graphs drawn in figure 1. The role of other diagrams with the radiative corrections will be discussed later. It can be shown that the planar ladder diagrams have the following asymptotical behavior (see [13] *e.g.*)

$$T^{plan}(s,t) \sim c\,s\,\ln^n(s)\,\phi(t), \tag{2}$$

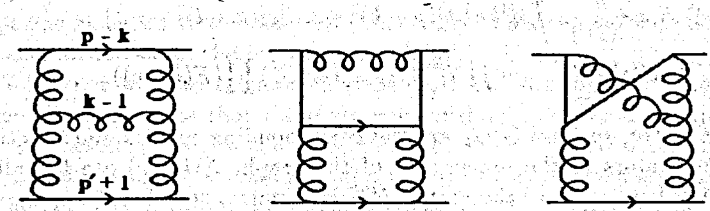

(a) (b) (c)

Figure 1: The α_s^3 contributions to the spin-flip amplitude

where c is a color factor. Moreover, there are $s \to u$ crossing diagrams with crossed gluon lines. It is easy to see that the color factors in these cases are the same for the color singlet state in the t-channel. In the semi-hard region we have $u \simeq -s$ and the real parts are compensated in the sum of diagrams. As a result, we obtain

$$T^{plan}(s,t) + T^{s \to u}(s,t) \simeq ics\, n\pi \ln^{n-1}(s)\,\phi(t). \tag{3}$$

So we can calculate only the imaginary parts of diagrams in the case of pomeron exchange.

In calculations we shall use the Feynman gauge because only the $g_{\mu,\nu}$ terms in t-channel gluon propagators contribute to the leading $\sim s$ terms of the scattering amplitudes and in the α_s^3 order we have no ghost contributions. Let us calculate the matrix element of the amplitude, Fig.1, with spin-flip in the upper quark line. In this case only the spin-non-flip matrix element in the lower quark line has a term growing as s for $s \to \infty$. It is determined by the following structure [8]

$$\bar{u}^+(p'+r)\gamma^\mu(\not{p}' + \not{l} + m)\gamma^\nu u^+(p'-r) \simeq 4p'^\mu p'^\nu. \tag{4}$$

To show that the spin-flip and non-flip amplitudes have a similar asymptotics as $s \to \infty$, we shall write the matrix structure in the upper quark line for the diagram of Fig.1b as an example:

$$\begin{gathered} N_b^{\mu,\nu} 4p'_\mu p'_\nu = 4\gamma_\rho(\not{k} - \not{r} + m)\not{p}'(\not{k} - \not{l} + m)\not{p}'(\not{k} + \not{r} + m)\gamma^\rho \simeq \\ 16(kp')\{\not{p}'[k^2 - r^2 - m^2] - 2[(kp')\not{k} - 2m(kp') + i\epsilon^{\alpha\lambda\mu\sigma}k_\alpha p'_\lambda r_\mu \gamma_\sigma\gamma_5]\}. \end{gathered} \tag{5}$$

Here we omit the terms proportional to (lp') which do not contribute to the leading asymptotic of the numerator (5). It is easy to see that the term proportional to $\not{p}'$ in (5) can lead only to the spin-non-flip amplitude but all other terms produce the spin-flip one. Moreover, the direct calculation of the matrix elements with the help of the results from [8] shows that both flip and non-flip amplitudes are growing as s^2 in the $s \to \infty$ limit. So they are of the same order of magnitude.

Now let us calculate the imaginary parts of the spin-non-flip matrix elements in the lower quark line $\langle T_i(s,t)\rangle$ (see (4)) of the diagrams in Fig.1(a)-(c). They have the form

$$\begin{gathered} \mathrm{Im}\langle T_i(s,t)\rangle = c_i \frac{g^6}{2(2\pi)^5} \int d^4k d^4l \delta[(p-k)^2 - m_1^2]\delta[(k-l)^2 - m_2^2] \\ \delta[(p'+l)^2 - m^2]\,[N_i^{\mu\nu} 4p'_\mu p'_\nu]\,(G_i^1 G_i^2) \prod (F(l \pm r)), \end{gathered} \tag{6}$$

where c_i is a color factor, m_i and $G_i^1 G_i^2$ are the corresponding masses and functions from t-channel propagators in the upper part of the graph, $F(l \pm r)$ are the gluon propagators from the lower part of the graph, $N_i^{\mu\nu}$ is a matrix structure in the upper quark line. It is useful to perform the calculations in the light-cone variables

$$k = (xp_+, k_-, k_\perp),\ l = (yp_+, l_-, l_\perp),\ p_\pm = p_0 \pm p_z.$$

After integration with the δ-functions we obtain the following representation

$$\begin{gathered} \mathrm{Im}\langle T_i(s,t)\rangle = c_i \frac{\alpha_s^3}{(2\pi)^2 s} \int_{s_0/s}^1 \frac{dx}{x(1-x)} \int d^2k_\perp d^2l_\perp \\ \left[N_i^{\mu\nu} 4p'_\mu p'_\nu\ (G_i^1 G_i^2) \prod (F(l \pm r))\right] |_{k_-, l_-, q_-, y}. \end{gathered} \tag{7}$$

Here k_-, l_-, y are pole solutions of the δ-functions. For the investigated diagrams the functions G and F look as follows

$$\begin{gathered} G_a^{1,2} = G_a^\pm = -\frac{1-x}{x^2m^2 + (1-x)\lambda^2 + [k_\perp \pm (1-x)r_\perp]^2}; \\ G_b^{1,2} = -\frac{1-x}{(1-x)^2m^2 + x\lambda^2 + [k_\perp \pm (1-x)r_\perp]^2}; \\ G_c^1 = G_a^+,\ G_c^2 = -\frac{x}{x^2m^2 + (1-x)\lambda^2 + [k_\perp - l_\perp + xr_\perp]^2}; \\ F(l \pm r) = -\frac{1}{\lambda^2 + [l_\perp \pm r_\perp]^2}, \end{gathered} \tag{8}$$

where we introduce the mass λ in the gluon propagators. It follows from (8) that in the $\lambda \to 0$ limit we have infrared singularities only from the gluon propagators $F(l \pm r)$ in the lower part of the graph. All other propagators have no divergences in this limit.

The numerators of the diagrams can be decomposed over the independent matrix structures

$$N_i^{\mu\nu} 4p'_\mu p'_\nu = \sum_{k=0}^4 N_i^k \hat{\Gamma}_k. \tag{9}$$

Here we use the following definitions of these matrix structures

$$\hat{\Gamma}_0 = \frac{\not{p}'}{s},\ \hat{\Gamma}_1 = I,\ \hat{\Gamma}_2 = \not{p},\ \hat{\Gamma}_3 = \frac{i\epsilon^{\alpha\beta\gamma\rho}p_\alpha p'_\beta r_\gamma \gamma_\rho\gamma_5}{s},\ \hat{\Gamma}_4 = \frac{im\sigma^{\alpha\beta}p'_\alpha r_\beta}{s}. \tag{10}$$

As a result of such normalization in (10) we have no energy dependences in the spin-flip and non-flip matrix elements of $\langle\hat{\Gamma}_i\rangle$. It was mentioned when we analysed the matrix structure of (5) that the $\hat{\Gamma}_0$ term contributes only to the spin-non-flip amplitude in the upper quark line. The $\hat{\Gamma}_1, \hat{\Gamma}_2$ structures contributes to both the spin-flip and non-flip amplitudes. The structures $\hat{\Gamma}_3, \hat{\Gamma}_4$ are determined by the antisymmetric terms in the quark line and lead to the spin-flip effects only. This can be checked, for example, by a direct calculation of the matrix elements [8].

We do not want to calculate here the spin-non-flip amplitude connected with the $\hat{\Gamma}_0$ contribution. Note that there are nonvanishing parts in the limit $x \to 0$ at N_i^0 in (9). As a result, the main contribution to the integral (7) is determined by the region $x \sim s_0/s$ that leads to the additional $ln(s/s_0)$ factor. Just these terms were calculated in different papers (see [13] e.g.) in the leading log approximation. We shall analyse the $\hat{\Gamma}_1 - \hat{\Gamma}_4$ effects here. They do not have the $ln(s/s_0)$ factor and have been omitted in the previous calculations. The forms of the leading terms with respect to s of N_i^k in (9) together with the spin-flip matrix elements $\langle N_i^{\mu\nu} 4p'_\mu p'_\nu\rangle_{flip}$ for the graphs of Fig.1

	A	B	C
N^1	$10\,m\,s^2\,x^2$	$-16\,m\,s^2\,x^2$	$12\,m\,s^2\,x(1-x)$
N^2	$-8\,s^2\,x^2\,(1-x)$	$8\,s^2\,x^3$	$-8\,s^2\,x(1-x)^2$
N^3	$20\,s^2\,x(1-x)$	$16\,s^2\,x^2$	$4\,s^2\cdot$ $[(4x_i^2-7x+3)-(4x^2-10x+6)\,l_x/\Delta]$
N^4	$-20s^2\,x$	0	$-12s^2\cdot$ $[(1-2l_x/\Delta)(1-x)]$
$\langle N\rangle_{flip}$	$-8\,ms^2\cdot$ $\Delta\,x^2(1-x)$	$-8ms^2\cdot$ $\Delta\,x^2(1-x)$	$-4m\,s^2\cdot$ $x(1-x)\,[\Delta\,(1-2x)-2l_x]$

Table 1: The leading s^2 terms of the N_i amplitudes in (8) and the total spin-flip matrix elements $\langle N_i^{\mu\nu}4p'_\mu p'_\nu\rangle_{flip}$ for the diagrams of Fig.1a-c.

are shown in Table 1. All functions in the table are growing as s^2. One power of s is compensated in the integral (7) and both the spin-flip and non-flip amplitudes are growing as s.

The born two-gluon high-energy amplitude $O(\alpha_s^2)$ has a form

$$\langle T^{2g}(s,t)\rangle = A^{2g}(s,t)\hat{\Gamma}_0, \tag{11}$$

where

$$A^{2g}(s,t) = 4is\alpha_s^2 c_2 \int d^2l_\perp \prod(F(l\pm r)), \quad c_2=\frac{8}{36} \tag{12}$$

with $(F(l\pm r))$ determined in (8).

For the $\hat{\Gamma}_1-\Gamma_4$ contribution to the amplitudes Fig.1 we can write

$$\langle T_i(s,t)\rangle = \sum_{k=1}^{4} T_i^k(s,t)\,\hat{\Gamma}_k, \tag{13}$$

It is easy to see that in $\langle T_a\rangle$ and $\langle T_b\rangle$ the integrals over $d^2k_\perp$ and $d^2l_\perp$ are factorized completely. Moreover, the integrals over $d^2l_\perp$ coincide with the transverse integral in (12). So, we have

$$\langle T_{a,b}(s,t)\rangle = A^{2g}(s,t)\sum_{k=1}^{4} B_{a,b}^k\,\hat{\Gamma}_k = A^{2g}(s,t)\,\hat{B}_{a,b}. \tag{14}$$

This factorization can be proved for the $\langle T_c\rangle$ term on the basis of some approximations only and we use (14) as a definition for B_c

$$\langle T_c(s,t)\rangle = A^{2g}(s,t)\,\hat{B}_c. \tag{15}$$

For the sum of (11) and the amplitudes from Fig.1 we can write

$$\langle T(s,t)\rangle = A^{2g}(s,t)\,[\hat{\Gamma}_0 + \sum_{i=a..c}\hat{B}_i]. \tag{16}$$

Calculating the spin-non-flip and spin-flip matrix elements in the upper quark line from (16) we have

$$\langle T(s,t)\rangle_{non-flip} = A^{2g}(s,t)\,(1+O(\alpha_s)),$$
$$\langle T(s,t)\rangle_{flip} = A^{2g}(s,t)\sum_{i=a..c}\langle\hat{B}_i\rangle_{flip}. \tag{17}$$

As it was mentioned previously, in (17) we do not calculate the contribution of the α_s^3 terms to the $\langle T(s,t)\rangle_{non-flip}$.

The results of calculations of different spin-flip structures $B_{a,b}^k\langle\hat{\Gamma}_k\rangle_{flip}$ together with the full spin-flip amplitude $\langle\hat{B}_{a,b}\rangle_{flip}$ determined in (14) for the diagrams of Fig.1a,b are shown in Figure 2a,b. In calculation we use $\alpha_s=.3$ which is typical for $|q^2|=1GeV^2$ and $\lambda=.1GeV$. One can see that the individual contributions are not very small as compared to unity (the magnitude of the spin-non-flip amplitude after extracting the $A^{2g}(s,t)$ term). But they are different in sign and compensate each other essentially in the total amplitude. For example, the sum of the terms proportional to $\langle\hat{\Gamma}_1\rangle,\langle\hat{\Gamma}_3\rangle,\langle\Gamma_4\rangle$ is equal to zero and only $\langle\hat{\Gamma}_2\rangle$ contributes to the amplitude $\langle\hat{B}_a\rangle_{flip}$. The role of individual graphs (Fig.1) in the total spin-flip amplitude $\langle\hat{B}_i\rangle_{flip}$ is shown on Fig.2c. The magnitude of the nonplanar amplitude $\langle\hat{B}_c\rangle_{flip}$ is smaller than 10 per cent of the planar contributions. The total spin flip amplitude is about 2 per cent of the $\langle T(s,t)\rangle_{non-flip}$. The results of calculations do not depend practically on λ due to the nonsingular behavior of all propagators in the $d^2k_\perp$ integrals. Note that the smallness of the resulting spin-flip amplitude is caused by the compensation of different contributions, which is possible only for the quarks on the mass shell. Really, the model investigations of the γq elastic scattering at high energies [11, 12] show that the off-mass-shell effects in the quark loop increase the spin-flip amplitude essentially.

We analyse the role of the radiative corrections to the spin effects too. When we evaluate the leading s asymptotics of these amplitudes using the standard technique in the α representation, the further smallness $\sim\alpha\simeq 1/s$ occurs from the extra s- channel propagator. This small magnitude can be compensated by large scalar products in the numerator. This has happened for the spin-non-flip amplitude which behaves as $s\ln s$ [13]. However, such large terms are absent in the $\hat{\Gamma}_1-\hat{\Gamma}_4$ contributions and they are not growing as s. Thus the radiative graphs do not contribute to the leading asymptotic terms of the spin-flip amplitude. This result was confirmed by the numerical calculations.

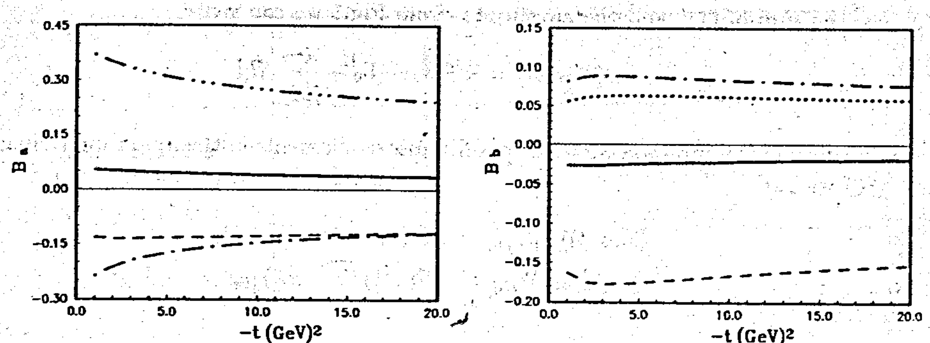

(a) (b)

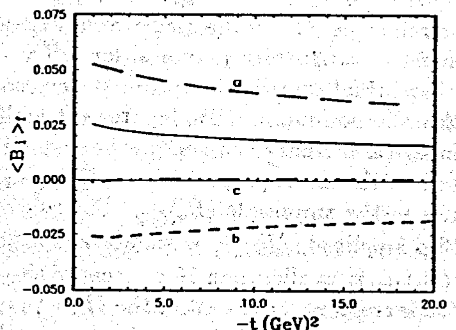

(c)

Fig.2 (a,b) The contributions of the different structures $<\hat{B}^{soft}>_{flip}$ of the diagrams Fig.1a,b: full curve - the total spin-flip amplitudes; contributions of the different structures: broken curve - for the Γ_1, dots - for the Γ_2, dotted line - for the Γ_3, dots-dash - for the Γ_4

Fig.2 (c) The spin-flip amplitudes $<\hat{B}^{soft}_{a-c}>_{flip}$ (marked by a - c); full curve - sum of the amplitudes

So we see that the diagrams, Fig.1a,b, determine the high energy contribution to the spin-flip amplitude. It was shown previously that we have a full factorization of the transverse integrals in these terms. As a result, the amplitude $\hat{B}$ in (14,16) contains only the integration over $d^2k_\perp$ from the sum of the upper parts of graphs, Fig.1a,b. All momenta in these subgraphs are about p (p' components are suppressed by s). Thus these parts of diagrams are at low energies because we cannot obtain any large magnitude $\sim s$ from the scalar products of the momenta. This leads us to the conclusion that we obtain the factorization of high energy (A^{2g}) and low energy (B) contributions in the spin-flip amplitude in the α_s^3 order

$$\langle T_{\alpha_s^3}(s,t)\rangle_{flip} = A^{2g}_{\alpha_s^2}(s,t)\langle\hat{B}(t)\rangle_{flip}. \tag{18}$$

We hope that the spin-flip amplitudes in higher α_s orders are determined by similar contributions, where the low-energy spin-flip part is the subgraph B near the valence quark. In this case the diagram must fall into two parts which are at low and high

energies

$$\langle T_{\alpha_s^{n+1}}(s,t)\rangle_{flip} = A^{2g}_{\alpha_s^n}(s,t)\langle\hat{B}(t)\rangle_{flip} \tag{19}$$

with the same $B(t)$ as in (18). Here $A^{2g}_{\alpha_s^n}(s,t)$ is a ladder two-gluon graph of the order α_s^n for qq high-energy scattering. In this case the spin-flip amplitude obtained as a result of the summation of these high energy pomeron graphs can be of the same energy behavior as the spin-non-flip amplitude

$$\frac{|T_{flip}|}{|T_{non-flip}|} \simeq \langle\hat{B}(t)\rangle_{flip}. \tag{20}$$

This quantity is of the order of α_s. However the consistent investigation of this problem is very complicated.

So, the gluons in the high energy ladder diagrams of qq elastic scattering at t-fixed make the spin-flip amplitude growing as s. This means the existence of the spin-flip part in pomeron exchange. It is shown that the main contribution in this case comes from the planar diagrams of the form, Fig.1a,b. The obtained results confirm the factorization in the spin-flip part of the pomeron exchange of the large-distance effects $\langle\hat{B}(t)\rangle_{flip}$ and the high energy spinless two gluon amplitude $A^{2g}(s,t)$. We observed this effect in our previous model investigations [11]. The ratio of the spin flip and non-flip amplitudes is not very large for the on-mass-shell quarks (only a few per cent), but this function can be energy-independent (20) or decrease only logarithmically with growing energy (1). The role of the off-mass-shell effects of the wave functions in the semi-hard region must be analysed in future investigations.

Acknowledgement. The authors express their deep gratitude to A.V.Efremov, V.A.Matveev, V.A.Meshcheryakov and O.V.Teryaev for fruitful discussions.

References

[1] S.B. Nurushev, Proc. of the 2 Int. Workshop on High Energy Spin Phys. p 5 (Protvino, 1984)
A.D.Krish, Proc. of the 6 Int. Symp. on High Energy Spin Phys. p C2-511 (Marseille,1984)
N.E.Tyurin, Proc. of the 8 Int. Symp. on High Energy Spin Phys. p 65 (Bonn,1990).

[2] S.J.Brodsky, G.P.Lepage, Phys.Rev. 1980, **D22**, 2157.

[3] E.A.Kuraev, L.N.Lipatov, S.V.Fadin, Zh.Eksp.Teor.Fiz., 1977, **72**, 377.

[4] F.E.Low, Phys.Rev., 1975, **D12**, 163;
S.Nussinov, Phys.Rev.Lett., 1975, **34**, 1286.

[5] P.V.Landshoff, O. Nachtmann, Z.Phys.C-Particles and Fields 1987, **35**, 405.

[6] A.Donnachie, P.V.Landshoff, Nucl.Phys., 1989, **B311** 509.

[7] D.A.Ross, J.Phys.G:Nucl.Part.Phys., 1989, **15**, 1175.

[8] S.V.Goloskokov, Yad.Fis., 1989, **49**, 1427.

[9] S.V.Goloskokov, Yad.Fis., 1990, **52**, 246.

[10] S.V.Goloskokov, Z.Phys. C-Particles and Fields 1991, **52**, 329.

[11] S.V.Goloskokov, J.Phys. G:Nucl.Part.Phys., 1993, **19**, 67.

[12] S.V.Goloskokov, Pisa prepr. IFUP-TH 23/92, Pisa, 1992.

[13] B.M.McCoy, T.T.Wu, Phys.Rev., 1975,**D12**, 3257;
H.T.Nich, Y.P.Yao, Phys.Rev., 1976, **D13**, 1082;
L.Tybursky, Phys.Rev., 1976, **D13**, 1107.

**Received by Publishing Department
on May 11, 1993.**